Solvent structure and hydrodynamic effects in photoinduced electron transfer

S. F. Swallen, Kristin Weidemaier, and M. D. Fayer
Department of Chemistry, Stanford University, Stanford, California 94305

(Received 27 September 1995; accepted 16 November 1995)

A previously developed statistical mechanical theory describing photo-induced electron transfer and geminate recombination in liquid solutions has been modified to account for realistic finite-volume solvent effects. This work introduces physically important effects caused by the solvent which fundamentally affect the rates and spatial distribution of charge transfer events. The finite volume of solvent molecules gives rise to a nonuniform distribution of particles around an electron donor, which is incorporated into the theory by a two-particle radial distribution function (rdf). The Percus–Yevick solutions for the rdf can give numerically useful values for the solvent structure, $g(R)$ although any form of $g(R)$ can be used with the method. The nonuniform particle distribution significantly affects the electron transfer rates and the distribution of ion pairs formed by forward electron transfer, particularly at short times. In addition, finite solvent size affects the rate of relative diffusion between any donor–acceptor pair. These ''hydrodynamic effects'' slow down the interparticle diffusion rates when near contact, resulting in a major change in the long time behavior of photoexcited electron transfer systems. This work formally introduces the mathematical modifications to charge transfer theory necessary to account for the solvent structure and hydrodynamic effect and illustrates the results with model calculations. These calculations show that analysis of experiments with theories that do not include the rdf and hydrodynamic effects can result in significant errors in the interpretation of data. © *1996 American Institute of Physics.* [S0021-9606(96)02308-X]

I. INTRODUCTION

In liquid systems, time dependent ion pair formation resulting from photo-induced electron transfer has been examined and modeled with considerable success. This is especially true for intramolecular charge transfer.[1–4] The situation is much more complex, and understanding is more elusive, in systems of freely diffusing, independent molecules. The mathematical formalism required to account for diffusive particle motion in the context of photoinduced electron transfer and geminate recombination requires complex spatial averaging techniques. In the context of a three level system, in which there is a ground state neutral donor and neutral acceptors (DA), excited state donor and neutral acceptors (D^*A), and the charge transfer state consisting of a donor cation and an acceptor anion (D^+A^-), an exact solution to the time-dependent state probabilities has been presented.[5–9] (For concreteness, we will discuss the situation of initially neutral donor and acceptors undergoing electron transfer to form a cation and anion. The formalism can handle any other situation such as a doubly negatively charged donor transferring an electron to a neutral acceptor to form a donor anion and an acceptor anion.) In the previous presentations of the theory, the solvent was treated as a continuum and spatial transport of the molecules was by simple diffusion. Donor–acceptor and acceptor–acceptor excluded volume have been included,[10] but the continuum nature of the solvent meant that the solvent did not influence the spatial positions of the acceptors relative to the donor, nor did the solvent influence the nature of the diffusion.

Treating the solvent as a continuum is a standard approximation used in all theories of electron transfer in solution. However, there is nothing inherent in the exact treatment of the three level model that precludes a more realistic description of the solvent properties and the role that the molecular nature of the solvent plays in photoinduced electron transfer. In fact, as will be shown below, treating the solvent as a continuum leads to both quantitative and qualitative errors in the description of the dynamics of electron transfer.

The first important aspect of a realistic description of the solvent is that the finite physical volume of the solvent molecules results in a nonuniform particle distribution. When the volume of all the donor, acceptor, and solvent molecules are accounted for, the particle distribution is no longer spatially isotropic. Multiparticle interactions result in radially dependent density variations which deviate significantly from the continuum description. A tremendous amount of work has been invested in the study of particle correlations, and accurate methods of calculating the two-particle radial distribution function, $g(R)$, have been known for many years.[11–16] Because of the exquisitely sensitive distance dependence found in the electron transfer process, these spatial density variations can not be ignored. In this paper we introduce the mathematical formalism which permits these variations to be taken into account. For simplicity, a hard sphere model of $g(R)$ will be used. However, the formalism permits the inclusion of any model for the radial distribution function.

Another important aspect of real liquids that is important to the electron transfer problem is brought forward by studies of interparticle diffusion rates,[17–21] which have shown that

 0021-9606/96/104(8)/2976/11/$10.00

the magnitude of the diffusion coefficient is not a constant value, but is instead given by a distance dependent function. A single value of the diffusion constant, D, is only valid for large interparticle distances. In this limit, two particles move independently, and their diffusive motion is uncorrelated. However, when a pair approaches contact, their motions become correlated and specific events must occur in order for the two particles to move closer to each other. This influence, called the hydrodynamic effect,[17–21] greatly reduces the rate of approach between two specific molecules when separated by less than a few solvent shells. When they are nearly in contact, motion reducing the separation distance can only occur if intervening solvent molecules also undergo appropriate changes in position. If no direct path exists between the donor and an acceptor, the probability of the two diffusing closer together is significantly reduced. This obstruction effectively reduces the donor–acceptor interparticle diffusion constant when near contact. In a liquid, diffusive approach of acceptors to a photo-excited donor plays a major role in the rate of electron transfer, and therefore, the use of a single distance independent diffusion constant leads to an inaccurate description of the electron transfer dynamics. Several mathematical descriptions have been put forward to describe the spatial dependence of this effect.[19–21] The result of the diffusion constant being dependent on the radial separation of the molecules is to make the formal solution for interparticle electron transfer probability more complex. In this paper the hydrodynamic effect is introduced into the differential equations used to calculate the electron transfer probabilities.

In the following, the previous formalism is revised to include both hydrodynamic effects and the radial distribution function. Calculations are presented that illustrate the importance of these effects by comparison to calculations using the previously presented continuum theory. It should be noted that some concepts of this work have been examined by Northrup and Hynes.[21] These earlier works, based on previous suggestions by Smoluchowski[22] and Debye,[23] began a full fledged discussion of the general effects of a potential of mean force [due to solvent structure $g(R)$] and of the hydrodynamic effect of a distance dependent diffusion constant (due to solvent caging effects). These works, however, were limited to the basic Smoluchowski model of diffusion-limited reaction rates. They provide a preliminary analysis of the required concepts, but are limited by including multiparticle reactions only at contact. This paper introduces these concepts and extends them to a physically realistic model of through-solvent multiparticle electron transfer dynamics.

II. THEORY

A. Electron transfer in a continuum solvent

Considerable theoretical work has been performed previously to calculate the time-dependent photo-induced electron transfer observables in isotropic three-dimensional solid and liquid solutions.[5–24] The calculations, which will be summarized below, have produced exact expressions for $\langle P_{\mathrm{ex}}(t)\rangle$, the ensemble averaged probability that an initially photoexcited donor remains excited a time t after excitation, and for $\langle P_{\mathrm{ct}}(t)\rangle$, the ensemble averaged time dependent charge transfer state probability (probability of the existence of ion pairs). The model which this theory describes is a three level system; a ground state neutral donor surrounded by neutral acceptors (DA), a photo-excited donor and neutral acceptors (D*A), and the charge transfer ion pair state (D^+A^-). Electron donating chromophores are considered to be in sufficiently low concentration that there is no donor–donor excitation transfer. In addition, all ion pairs that are formed by forward transfer may only recombine geminately. The overall distance scales and energetics associated with photo-induced electron transfer makes this a reasonable assumption, although in some systems, electron hopping from an acceptor anion to a neutral acceptor could play a role. Electron hopping among acceptors is not included in the model. A discussion of this assumption of strict geminate recombination has been presented recently.[25]

The theoretical treatment of Refs. 6, 24, and most previous theoretical treatments of photo-induced electron transfer have taken the solvent to be a noninteracting continuum. As discussed in the Introduction, this led to the neglect of important aspects of the nature of real liquids that influence electron transfer. In the cases where the solvent structure and hydrodynamic effects have been examined, a model of molecular reaction which is not applicable to distance dependent electron transfer was examined.[21] To improve on this, it is important to account for noncontact through-solvent molecular reaction. The distance dependent rate of electron transfer from the excited donor to any acceptor located a distance R away is given by $k_f(R)$, while the geminate recombination rate is given by $k_b(R)$. The theory can handle any functional form of these rate parameters. Previous work has examined a monotonically decaying exponential,[5,6,24,26] as well as simpler descriptions such as the Collins and Kimball[27,28] and Smoluchowski models.[17,22] The exponential form of the rate parameter is expressed as

$$k_f(R)=\frac{1}{\tau}\exp\left(\frac{R_f-R}{a_f}\right),\quad k_b(R)=\frac{1}{\tau}\exp\left(\frac{R_b-R}{a_b}\right), \tag{1a}$$

where a_f and a_b are parameters defining the wave function overlap between the donor and acceptor molecules for forward and back transfer, respectively. R_f and R_b quantify the distance dependence of transfer events, and τ is the fluorescence lifetime of the excited donor. A more general and physically realistic form for the distance dependent transfer rate is given by the Marcus expression,[4,29,30]

$$k(R)=\frac{2\pi}{\hbar\sqrt{4\pi\lambda k_BT}}J_0^2\exp\left[\frac{-(\Delta G+\lambda)^2}{4\lambda k_BT}\right]\times\exp[-\beta(R-R_m)]. \tag{1b}$$

J_0 is the magnitude of the transfer matrix element, and β is the attenuation constant of the donor and acceptor wave function overlap. β is essentially the inverse of the wave-function overlap parameter given above, $1/a_f$. R_m is the

donor–acceptor contact distance. ΔG is the free energy change associated with electron transfer. The reorganization energy λ is expressed as[4,29]

$$\lambda = \frac{e^2}{2}\left(\frac{1}{\epsilon_{op}} - \frac{1}{\epsilon_s}\right)\left(\frac{1}{R_{don}} + \frac{1}{R_{acc}} - \frac{2}{r}\right), \tag{2}$$

where ϵ_{op} and ϵ_s are the optical and static solvent dielectric constants. R_{don} and R_{acc} are the van der Waals radii of the donor and acceptor.

The differential equations describing electron transfer in diffusive systems can be written, assuming a continuum solvent and non-interacting acceptor molecules, for the survival probability of the donor and a single acceptor,

$$\frac{\partial}{\partial t} S_{ex}(t|R_0) = D\nabla^2_{R_0} S_{ex}(t|R_0) - k_f(R_0) S_{ex}(t|R_0) \tag{3}$$

and for the ion (charge transfer) state,

$$\frac{\partial}{\partial t} S_{ct}(t|R_0) = L^+_{R_0} S_{ct}(t|R_0) - k_b(R_0) S_{ct}(t|R_0). \tag{4}$$

The solutions to Eqs. (3) and (4) are the probability that the donor still exists in the respective excited or cation state at time t after state formation, given an initial donor–acceptor separation R_0 at time $t=0$. For a spherically symmetric system, the diffusional operator $\nabla^2_{R_0}$ is defined as

$$\nabla^2_{R_0} = \frac{2}{R_0}\frac{\partial}{\partial R_0} + \frac{\partial^2}{\partial {R_0}^2} \tag{5}$$

and the Smoluchowski operator $L^+_{R_0}$ is

$$L^+_{R_0} = \frac{D}{R_0^2}\exp[-V(R_0)]\frac{\partial}{\partial R_0} R_0^2 \exp[V(R_0)]\frac{\partial}{\partial R_0}, \tag{6}$$

where $V(R_0)$ is the Coulomb potential between the donor cation and acceptor anion divided by kT, and D is the Fick diffusion coefficient. Both Eqs. (3) and (4) are solved with reflecting boundary conditions at the van der Waals contact distance between donor and acceptor. The solution for many acceptors for the probability of the donor remaining in the excited state at a time t after excitation has the form[31]

$$\langle P_{ex}(t)\rangle = \exp(-t/\tau) \times \exp\left\{-4\pi C \int_{R_m}^{\infty} [1 - S_{ex}(t|R_0)] R_0^2 dR_0\right\}. \tag{7}$$

The probability of being in the ion pair state at a time t after initial photoexcitation is[5,6]

$$\langle P_{ct}(t)\rangle = 4\pi C \int_{R_m}^{\infty}\int_0^t S_{ct}(t-t'|R_0) k_f(R_0) S_{ex}(t'|R_0) \times \langle P_{ex}(t')\rangle dt' R_0^2 dR_0. \tag{8}$$

The numerical solutions of Eqs. (7) and (8) are obtained by the Crank–Nicholson finite differencing method.[32,33,34] Thus, by means of numerical integration, it is possible to calculate exactly the time dependent electron transfer probability functions for the model described above. The results of this type of calculations have been compared to detailed Monte Carlo simulations, and found to be in complete agreement.[10] However, these results are for a continuum solvent. The molecular nature of the solvent will now be added to produce results that are more closely applicable to understanding experiments in real liquids.

B. Radial distribution function

The study of real liquids has shown that the spatial distribution of particles is not isotropic, but is significantly influenced by the excluded volume effects associated with finite particle size.[17,35,36,37] Experimental techniques, such as x-ray diffraction[38] and neutron scattering,[39,40] have shown a significant degree of local structure in room temperature liquids. The photo-induced electron transfer dynamics are influenced in two ways. The most obvious is the change in local acceptor concentration about a photo-excited donor. The probability of finding an acceptor at or very near to contact with the donor is significantly greater than it would be if the solvent were a continuum. In the latter case, the radial probability distribution, $p(R)$, goes as R^2dR. When account is taken of the repulsive part of the intermolecular potential, however, significant deviations from this average density are seen.[35,36,41] Mathematically, it is possible to account for these variations in the formalism by using the appropriate distribution function. This is given by

$$P(R)dR = g(R)p(R)dR = \frac{4\pi R^2}{\frac{4}{3}\pi R_v^3} g(R)dR,$$

where $p(R)$ is the probability distribution in a continuum, $g(R)$ is the liquid radial pair distribution function, and the denominator normalizes the distribution function. The value of R_v is the radial upper limit of the system. The model assumes an infinitely large volume centered about the donor, although this is limited for practical reasons to include only the volume necessary to reach convergence in the calculations. This value is chosen such that all electron transfer events and all relevant diffusive motion which occur on the time scale of interest are included. The new function $P(R)$ is used in place of the continuum distribution in Eq. (7) and (8). It should be noted that this probability expression is only valid in the limit of no acceptor–acceptor interaction. If the acceptor concentration is not too high (less than a few tenths molar), this form for $P(R)$ can be used with no loss of accuracy.[10]

The distance dependent solvent structure $g(R)$ is a static, time-independent function, and thus plays an additional role in the calculation of electron transfer functions. The diffusion of acceptor particles must allow for the motion of particles, yet maintain the overall liquid structure. In this way, the structure acts as a potential in solving the two-particle diffusion Eqs. (3) and (4).[17,19,21] Thus, both the forward (excited state) and back (charge transfer state) two particle survival probabilities take on the form of Eq. (4). In the forward

transfer, the potential of mean force is defined as $V(R)=-\ln[g(R)]$.[17,37] The back transfer potential additionally includes a Coulombic potential,

$$V(R)=-\ln[g(R)]+R_c/R,$$

where R_c is the Onsager radius. When including the solvent structure both in the diffusive potential term and in the probability distribution function, the final result for the excited state and charge transfer state probability functions, respectively, are

$$\langle P_{\rm ex}(t)\rangle=\exp(-t/\tau)\times\exp\left\{-4\pi C\int_{R_m}^{\infty}[1-S_{\rm ex}(t|R_0)]R_0^2 g(R_0)dR_0\right\}, \tag{9}$$

$$\langle P_{\rm ct}(t)\rangle=4\pi C\int_{R_m}^{\infty}\int_0^t S_{\rm ct}(t-t'|R_0)k_f(R_0)S_{\rm ex}(t'|R_0)\times\langle P_{\rm ex}(t')\rangle dt' R_0^2 g(R_0)dR_0. \tag{10}$$

As stated above, this formalism is exact in the limit of noninteracting acceptor molecules (no acceptor–acceptor excluded volume). The effects of acceptor–acceptor excluded volume have been studied previously.[10] For typical concentrations which exist in electron transfer experimental systems, i.e., up to a few tenths molar, acceptor–acceptor excluded volume can be neglected. At high concentrations, it can be treated approximately as described in Ref. 10.

Due to the importance of the radial distribution function (rdf) in describing many properties of liquids, a great deal of work has been done to obtain rdfs for different molecular sizes, densities, and geometries. The rdf for a liquid cannot be obtained exactly. A variety of numerical approximate methods for calculating rdfs have been developed, all with somewhat different accuracy under varying conditions. The most well known are the Kirkwood,[42] the Born–Green–Yvon,[43] the hypernetted chain,[44–46] and the Percus–Yevick equations.[11,47] Of these, the Percus–Yevick (PY) equation is generally considered to provide the most accurate rdfs.[35,37] Shortly after Percus and Yevick manipulated the Ornstein–Zernicke equation to obtain their nonlinear integral formula, Theile[12] and Wertheim[13] were able to obtain solutions to the PY form, giving the Laplace transform of the hard-sphere two-particle rdf. Further work has led to explicit analytical forms of the inverse-Laplace transform, allowing values of $g(R)$ to be more readily calculated.[14,48,49,50] All of the four integral equations can be used to obtain $g(R)$ under a variety of intermolecular potentials. The most commonly investigated potentials are the hard-sphere and Lennard-Jones 6-12 model.

In the calculation presented below, the PY method will be employed. Several points concerning the solutions to $g(R)$ must be noted. Foremost among these are the inaccuracies of the solutions to the PY equation. The most straightforward and commonly used solutions assume a hard-sphere intermolecular potential with no long range attractive forces. This leads to undercalculation of densities at contact, as well as slight misplacement of the density oscillations along the radial separation axis. In order to examine the work of Weeks, Chandler, and Andersen,[41] Verlet and Weis[16] were able to correct for these errors in large part. Throop and Bearman[51] have also examined the rdf obtained for the more realistic Lennard-Jones 6-12 potential. They found that while the magnitude of the peak heights were different than for the hard-sphere model, particularly at contact, the qualitative nature of the rdfs for the two potentials were similar.

In addition to these subtle corrections to the PY calculated values of $g(R)$, it is important to account for the inhomogeneity of the solution. The above calculations give the rdf for a homogeneous solution of particles with a uniform diameter. Leibowitz[15] was the first to obtain the Laplace transform solution for $g_i(R)$ for all species i in a hard-sphere mixture. Throop and Bearman[48] studied these results, giving a good qualitative and graphical description of $g(R)$ behavior in multicomponent solutions. Of particular importance for this current work was their analysis for low concentrations of solutes in a much higher density solvent. They found that the relevant criteria is the packing fraction, η_i, the percent of the total system volume occupied by the molecular specie i. The value of the packing fraction is given by $\eta=\pi\rho d^3/6$, where ρ is the number density and d is the molecular diameter. As the packing fraction ratio of solute to solvent becomes small, the functional form of $g_i(R)$ for each solute i corresponds to the $g(R)$ obtained for a homogeneous one-component fluid of spheres with radius equal to that of the solvent. For many intermolecular electron transfer experiments, where solute to solvent packing fraction ratios are less than 0.1 (a few tenths molar), this is an excellent approximation. This simplifies the calculation of the rdf necessary to describe most experimental electron transfer systems. Values for $g(R)$ for a single component liquid of solvent molecules can be obtained via Refs. 14, 18, and corrected according to Verlet and Weis.[16] The hard-sphere contact distance is then obtained from the sum of the donor and acceptor radii. In this way, one obtains $g(R)$ results which, as a first approximation, are in excellent agreement with experimental measurements and simulations.

More subtle issues concerning the accuracy of the two-particle hard sphere model have also been examined. Studies of rdfs for nonspherical molecules have included simulations and theoretical approaches for geometries such as ellipsoids[52] and spherocyliders.[53] Also, theoretical work has focused on including more than the simple two-particle interactions. Alder,[54] Attard,[55] and Stell[56] have looked at $g(R)$ values when considering both two and three particle direct interactions. These more extensive refinements represent only small changes in the $g(R)$ functions.

For the purposes of this paper, the most important point is that the formalism can employ any form of $g(R)$. Here, the hard sphere $g(R)$ will be used. This will be sufficient to show the profound changes that occur when a reasonable $g(R)$ replaces the continuum model that has been employed previously in studies of photo-induced electron transfer. While real liquids are not hard spheres, the liquid structure is dominated by the steep repulsive part of the potential.[35,41]

Therefore, in addition to showing qualitative features of the electron transfer problem, the hard sphere model should be capable of providing a reasonable, quantitatively accurate description of experimental systems. More accurate forms of $g(R)$ can be used if experimental results indicate that it is necessary.

C. The hydrodynamic effect

The diffusion of two particles in solution is not uniform for any radial separation, but is instead a function of the separation distance.[17,19,20,21] Fluid flow studies have shown that two bodies widely removed from each other have uncorrelated motions, and the relative rates of diffusion are equal to the sum of the two self-diffusion coefficients in an infinite bath. However, the picture is different when two particles, such as an electron donor and acceptor, approach contact. In this case, the hydrodynamic effect becomes significant, and the mutual diffusion rate is substantially decreased.[17,19,20,21] For the two particles to move closer together when they are already near contact, any obstructing solvent molecules must be forced to vacate the intervening space. The finite volume of the two particles acts to reduce the available paths of escape for the solvent, effectively decreasing the interparticle diffusion rate. In electron transfer systems, where most of the reactions are occurring near contact, the hydrodynamic effect can be significant.

The inclusion of a distance-dependent diffusion constant in the existing statistical mechanical treatment of electron transfer can be accomplished with only minor changes in the mathematical formalism. As stated above, when the solvent structure $g(R)$ is included, the form of Eq. (3) for the excited state pair survival probability is not applicable. Instead, both the excited and charge transfer state pair probabilities must be obtained via Eq. (4), using the appropriate form of the interparticle potential $V(R)$. With the inclusion of a distance dependent diffusion constant, the Smoluchowski operator in Eq. (4) must be modified to read,

$$L^{+}_{R_0} = \frac{1}{R_0^2}\exp[-V(R_0)]\,\frac{\partial}{\partial R_0}\,D(R)R_0^2 \times \exp[V(R_0)]\,\frac{\partial}{\partial R_0}. \tag{11}$$

This requires no formal changes in the expressions for the ensemble averaged excited state and charge transfer state probabilities $\langle P_{\rm ex}(t)\rangle$ and $\langle P_{\rm ct}(t)\rangle$, given by Eqs. (9) and (10), respectively. The only changes required are to include the $D(R)$ term in the finite differencing technique when obtaining numerical solutions to the pair survival probability functions $S_{\rm ex}(t|R_0)$ and $S_{\rm ct}(t|R_0)$.

The exact range of hydrodynamic repulsion is uncertain. Analytical approximations for the radial dependence of the diffusion coefficient have been presented in several different forms.[19,20,21] Typically, these have been expressions which have been found to agree reasonably with empirical evidence. The general form of all these functions is based on a maximum value of the diffusion coefficient, which $D(R)$ approaches asymptotically in the limit of large particle separation R, while the function monotonically decreases with smaller radial separation. The classical expression for the distance dependence has the form $D(R)=D(1-l/R)$, where $l=(3a_1a_2/a_1+a_2)$, a_1 and a_2 are the radii of the molecules under consideration, and D is the Fick diffusion coefficient in the Stokes continuum limit. In the case of equal sized solute molecules ($a_1=a_2$), the diffusion coefficient at contact is one fourth the magnitude of the coefficient in the continuum limit. Deutch and Felderhof[19] also predict similar results assuming "stick" boundary conditions. Wolynes and Deutch[20] have pointed out that stick boundary conditions are only appropriate when the solute molecules are much larger than the surrounding solvent. In the limit of roughly equal solute and solvent radii, slip boundary conditions are considered more realistic. This suggests that the classical expression gives a perturbation in D which overestimates the range and magnitude of the hydrodynamic effect. Rather than a value of $D(R)=D/4$ obtained at contact for the previously mentioned classical expression, Wolynes and Deutch obtain a value of $D/2$ at contact using slip boundary conditions. Northrup and Hynes[21] presented an approximate form which is qualitatively similar to the analysis of Wolynes and Deutch, and is now commonly used,

$$D(R)=D\left[1-\tfrac{1}{2}\exp\left(\frac{R_m-R}{R_m}\right)\right], \tag{12}$$

where R_m is the contact distance between two particles for which the diffusion of interest is occurring. Northrup and Hynes incorporated this distance dependent diffusion coefficient into the Smoluchowski theory of diffusion controlled reaction rates. They found it to be an appropriate, albeit somewhat approximate, means of including the solvent caging effects on interparticle diffusion. Their results predicted only a modest change in the Smoluchowski rate constants due to hydrodynamic effects.

Calculations based on the Smoluchowski model, however, do not provide a realistic picture of electron transfer in liquids. It is important to include through-solvent molecular interactions in the manner presented in Sec. II A. The results presented below were calculated using Eq. (12) as the form of the diffusion coefficient when considering the diffusion of both the neutral excited state reactants, as well as the charge transfer state ions. Other forms of the diffusion coefficient may be used interchangeably in the theory presented above for electron transfer state probabilities. These uncertainties in the functional form of $D(R)$ should not belie the fact that the hydrodynamic effect plays a significant role in the intermolecular diffusion rates of reactants. All of the mentioned models of the effect describe the same basic behavior of decreased diffusive motion when near contact, and therefore it is important to include this effect in diffusion-influenced reactions such as electron transfer.

III. RESULTS

Experimental studies have used the statistical mechanical theory described in Sec. II A, i.e., the continuum theory, to analyze both forward and back transfer data.[24,26] In these previous analyses of the forward transfer data, the exponential form of the rate parameter, $k_f(R)$, was used, giving explicit values for the transfer parameters a_f and R_f. The magnitudes of these parameters suggested that, within the limits of the continuum model, electron transfer was an extremely short range process. The vast majority of transfer events occurred within 1 Å of contact between donor and acceptor. Values for the electronic wave function overlap, a_f, were found to be approximately 0.25 Å, which corresponds to the inverse of β in the Marcus form of $k_f(R)$, giving values of β of roughly 4.0 $Å^{-1}$. Although it is unclear if there have been any realistic measurements of β in through-solvent photoinduced electron transfer systems, these values of β are larger than would be expected based on other types of experiments and on knowledge of the basic principles of electron transfer.[2,30,57]

To appreciate the ramifications of the various physical elements of the theory presented above, each of the theoretical methods introduced in Sec. II will be investigated separately. The inclusion of the solvent structure $g(R)$ significantly alters the local density of acceptors about a photoexcited donor compared to the average density which appears in the continuum model. The concentration of acceptors oscillates about the average density and converges to the average density at large distance. Since electron transfer is short range, the deviations from the average density of acceptors in this region are significant. For the hard sphere model, the largest magnitude change in local density occurs exactly at contact. Depending on the overall system density, this variation may be more than a factor of 5 times the average bulk density.[14,48] This effect is somewhat counterweighted by values which are less than the average at roughly odd numbers of the solvent radius. If the exponential form [Eq. (1a)] of the distance dependent transfer rate is used, it decreases monotonically away from contact. With the Marcus form [Eq. (1b)], for most transfer parameter values in the normal region, the transfer rate also decreases monotonically. However, it is possible with the Marcus model for the transfer rate to initially increase with increasing donor–acceptor separation. Regardless, the electron transfer rate is changing rapidly with distance in precisely the same region where the concentration of acceptors is undergoing its largest deviations from the average.

The effect that $g(R)$ has on the ensemble averaged photo-induced electron transfer dynamics can be seen clearly in Figs. 1 and 2. The insets show the short time behavior on an expanded scale. The calculations were performed using the Marcus model of the distance dependent transfer rate, with the parameters given in the figure caption. Figure 1 shows excited state $\langle P_{ex}(t)\rangle$ curves, calculated for one set of transfer parameters, by 4 different methods. (a) The simple model with no solvent structural effects; (b) including only the radial distribution function $g(R)$; (c) including only the hydrodynamic effect $D(R)$; and (d) the full detailed model with both $g(R)$ and $D(R)$. A fluorescence decay lifetime was not included in these calculations in order to emphasize the influence of each effect. A lifetime can be included by multiplying each curve by an exponential decay, and does not change the qualitative behavior of the models. Figure 2 shows charge transfer state $\langle P_{ct}(t)\rangle$ curves for a single set of forward and back transfer parameters, generated by the same four methods used in Fig. 1. In this case, an excited state fluorescence lifetime of 15.0 ns has been included in the calculations. This is required for the back transfer curves to be physically meaningful, because the lifetime is no longer simply a multiplicitive factor. Instead, it is fully integrated into the ensemble averages which give $\langle P_{ct}(t)\rangle$.

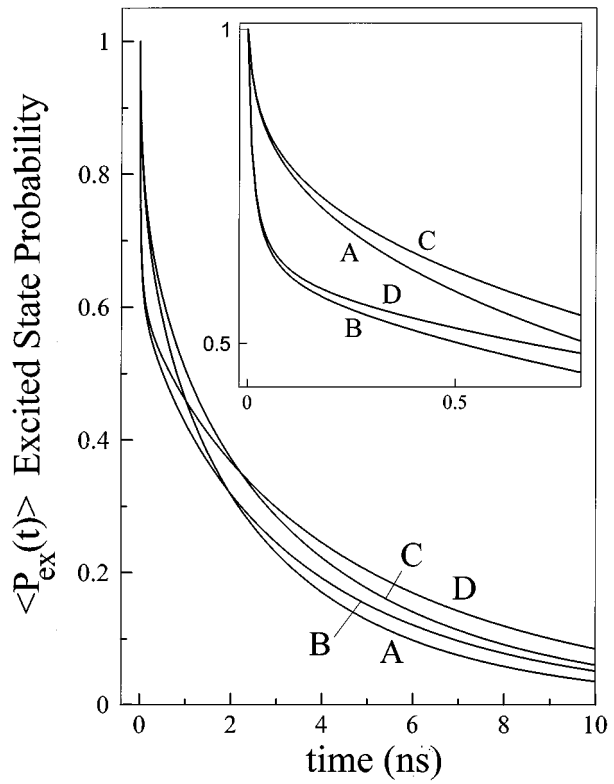

FIG. 1. Excited state probability $\langle P_{ex}(t)\rangle$ calculated for one set of electron transfer parameters using varying degrees of complexity of the theoretical model. All curves use the Marcus form of the rate parameter $k_f(R)$, where $J_0=40$ cm^{-1}, $\beta=1.0$ $Å^{-1}$, $\Delta G=-0.4$ eV. The Fick diffusion constant $D=20.0$ $Å^2$/ns, the acceptor concentration is 0.1 M, and a donor–acceptor contact distance $R_m=9.0$ Å. Curve A is generated using the simple model of electron transfer, with no solvent interactions. Curve B includes a solvent structure factor $g(R)$ (50% packing fraction, 9.0 Å diam). Curve C includes only the hydrodynamic effect $D(R)$ from Eq. (12), while curve D includes both $g(R)$ and $D(R)$. The solvent dielectric values are $\epsilon_{op}=2.0$, $\epsilon_s=8.0$. The inset shows the short time behavior of all four curves A–D.

The curves labeled A in Figs. 1 and 2 are excited state and charge transfer state calculations, respectively, for the continuum case, i.e., no radial distribution function, and a distance independent diffusion coefficient, $D(R)=D$. These are solutions obtained directly from Eqs. (7) and (8). The curves labeled B in both figures give $\langle P_{ex}(t)\rangle$ and $\langle P_{ct}(t)\rangle$, respectively, for calculations which include a hard-sphere

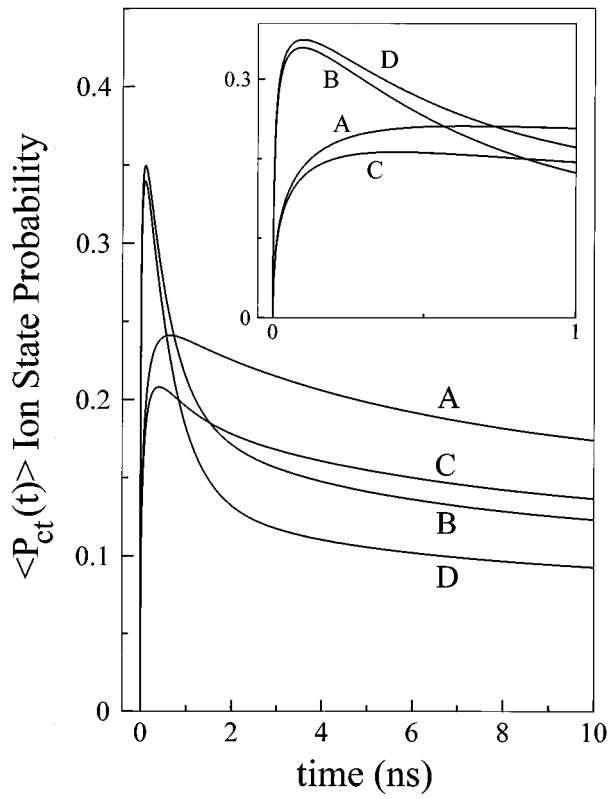

FIG. 2. Charge transfer state probability $\langle P_{ct}(t)\rangle$ for one set of electron transfer parameters, using varying degrees of complexity of the electron transfer model. The Fick diffusion constant $D=20.0$ Å^2/ns, the acceptor concentration is 0.1 M, the donor–acceptor contact distance $R_m=9.0$ Å, and the fluorescence lifetime $\tau=15.0$ ns. The forward transfer parameters are $J_0=40$ cm^{-1}, $\beta=1.7$ Å^{-1}, $\Delta G=-0.6$ eV. The back transfer parameters are $J_0=100$ cm^{-1}, $\beta=1.0$ Å^{-1}, $\Delta G=-1.0$ eV. Curve A is the simple form of the model, B includes the solvent structure $g(R)$ (50% packing fraction, 9.0 Å diam), C includes the hydrodynamic effect $D(R)$, and curve D includes both $g(R)$ and $D(R)$. The solvent dielectric values are $\epsilon_{op}=2.0$, $\epsilon_s=8.0$. No Coulomb potential is used in the ion diffusion calculations. The excited state fluorescence lifetime $\tau=15.0$ ns. The inset shows the short time behavior of all four curves A–D.

$g(R)$. The inclusion of solvent structure causes a dramatic increase in the rates of both forward and back electron transfer at short times. This short time behavior is dominated by donors with nearby acceptors that are likely to undergo transfer rapidly. Due to the significant increase in acceptor density at short distance, the overall likelihood of a donor being quenched is increased dramatically. The qualitative effects seen in Figs. 1 and 2 occur for any choice of transfer parameters. The magnitude of the difference between the simple model with no solvent structure effects and the detailed model is somewhat dependent on the values of J_0 and β, as well as the diffusion coefficient D. For extremely fast rates, local density fluctuations become somewhat less important because most donors will have at least one acceptor close enough to undergo rapid transfer. Even in this situation, the detailed time dependence is substantially modified. From Figs. 1 and 2 it is clear that solvent structure must be accounted for in any physically reasonable theory.

While both the hydrodynamic effect and the solvent structure have their genesis in the finite volume of solvent particles, their influence on the rates of electron transfer are quite different. In contrast to the influence of $g(R)$, the hydrodynamic effect tends to slow down the overall rate of electron transfer. When near contact, the local rate of diffusion between a donor and acceptor is greatly reduced. This acts to limit the probability of close encounter between two possible neutral reactants, thereby reducing the rate of transfer events. The curves labeled C in Figs. 1 and 2 show the excited and charge transfer state probability curves calculated using a distance dependent term $D(R)$ given by Eq. (12). No solvent structure $g(R)$ is included. The values for the transfer parameters are the same as for curves A and B. Comparing curves A and C, it is seen that the probability of forward transfer at all but the shortest times is decreased. The effect on the back transfer kinetics is more pronounced. By limiting the rates of approach via diffusion, donor and acceptor molecules are less likely to interact. It should be noted that at very short times, this effect is not important because diffusion does not play a significant role in transfer dynamics. On the one picosecond time scale, only donors and acceptors which are already near each other will interact. The magnitude of the influence of the hydrodynamic effect is inversely related to the viscosity of the bulk solvent, and vanishes in solid, glassy solution.

To correctly model a real system, both the solvent structure $g(R)$ and hydrodynamic effect $D(R)$ must be included simultaneously. The curves labeled D in Figs. 1 and 2 give the excited and charge transfer state probabilities, respectively, for the complete theory. The transfer parameters are the same as for curves A–C. Comparison of curves A and D shows the difference between the simple continuum theory and the full detailed theory that accounts for the molecular properties of the solvent. The interesting behavior of the calculations arises from the timescales of influence of the two effects. As mentioned above, the solvent structure is most important at short times and short distances. Conversely, the hydrodynamic effect becomes more important at longer times, and acts to slow down the observed kinetics. Comparing curves A and D, the results of the full theory are fundamentally different from what is obtained with the simple continuum theory. The significant disparities in the functional forms of the probability curves will play an important role in examining data from experimental systems.

In addition to the solvent structure affecting the probabilities of forward and back transfer, the inclusion of the radial distribution function may, under certain conditions, lead to $\langle P_{ct}(t)\rangle$ curves with a functionally different short time behavior than is seen with the simple model. Figure 3 displays the charge transfer state probability for one set of parameters which exhibits a separation of ion formation and geminate recombination into two discrete time scales in the presence of the radial distribution function (curve B), while this separation of time scales is not observed in the simple model (curve A). Inclusion of the hydrodynamic effect does not change the qualitative behavior of curve B in this short time regime. The extremely rapid generation of ions is due to the high local density of acceptors near to contact with the

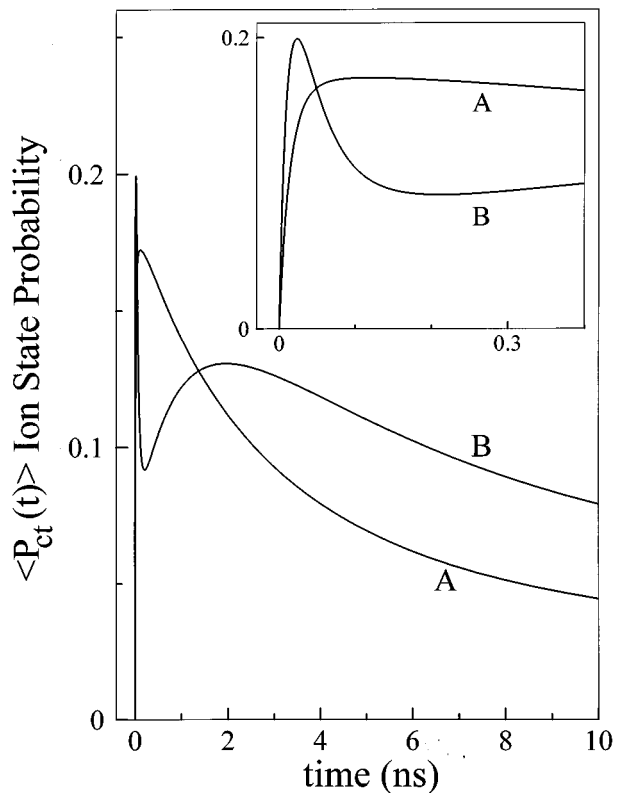

FIG. 3. Charge transfer state probability $\langle P_{ct}(t)\rangle$ for one set of electron transfer parameters, comparing the simple and detailed models. The Fick diffusion constant $D=20.0$ Å^2/ns, the acceptor concentration is 0.1 M, the donor–acceptor contact distance $R_m=9.0$ Å, and the fluorescence lifetime $\tau=15.0$ ns. The forward transfer parameters are $J_0=40$ cm^{-1}, $\beta=1.0$ Å^{-1}, $\Delta G=-1.0$ eV. The back transfer parameters are $J_0=60$ cm^{-1}, $\beta=1.5$ Å^{-1}, $\Delta G=-1.1$ eV. Curve A is the simple form of the model, and B is the detailed model including both $g(R)$ (50% packing fraction, 9.0 Å diam) and $D(R)$. The solvent dielectric values are $\epsilon_{op}=2.0$, $\epsilon_s=8.0$. An Onsager length of 50 Å is used in the ion diffusion calculations. The inset shows the short time behavior of both curves.

donor, caused by the solvent structure. However, because these ions are formed at such small separations, the rate of back transfer is also quite rapid. This causes the value of $\langle P_{ct}(t)\rangle$ to peak at very short time, then decay very quickly. Interestingly, this short time behavior is functionally separated from the long time (nanosecond) generation of ions brought about by longer range transfer events and diffusional motion. The short time regime is displayed on an expanded scale in the inset to Fig. 3. This time scale separation is due to the oscillatory variations in the local density caused by the solvent structure. While a high density near contact enhances short range (and thus short time) transfer, the opposite effect is seen at slightly longer distances, because the solvent density is significantly reduced below the average in the spatial region just outside of contact. This depletion of acceptor density at moderate distances ($\sim$3 molecular radii) decreases the probability of an ion being formed at that separation, as well as decreases the likelihood of an acceptor diffusing in toward the excited donor when initially at large separation. For these reasons, the probability of transfer to moderate distances is low, and on moderate time scales the rate of ion formation is much less than would be expected in a structureless continuum. These effects are reduced in the limit of long time, as diffusion and longer range transfer events become more important factors.

This separation of distance and time scales for electron transfer is affected by the values of the transfer parameters, the form of the solvent structure, and the value of the diffusion coefficient D. The behavior seen in Fig. 3 for $\langle P_{ct}(t)\rangle$ is not observed in all cases. For many sets of parameters which give fast transfer, an initial rise and then monotonic decay is seen in the charge transfer state probability, such as Fig. 2. It is possible that experimental systems will exhibit this short time functional form.

In deference to the difficulty required to reach numerical convergence in all the above calculations, extensive Monte Carlo simulations were carried out for the same system parameters. Details of the simulations for liquids and solids have been presented previously.[10,25] For all values of the transfer parameters, diffusion coefficient, acceptor concentration, and radial distribution function, the simulations reproduced the excited and ion state calculations on all time scales. For values such as those given in Fig. 3, the simulations perfectly reproduced the rapid creation and loss of ion population, followed by the long time regeneration of the ion state. Thus it is clear that the short time behavior of these systems is not a numerical discrepancy, but rather is a direct result of the physical nature of the solvent, and is to be expected for some values of the electron transfer parameters.

In order to further study the effects of including the physically realistic radial distribution and hydrodynamic terms, more in-depth comparisons were made between the simple (continuum solvent) and detailed (full solvent description) models. Excited state probability curves were generated using the detailed theory containing both $g(R)$ and $D(R)$ for various concentrations and transfer parameters, and then fits to these theoretical curves were obtained using the simple theory with no solvent effects. Figure 4 gives $\langle P_{ex}(t)\rangle$ curves for three concentrations of acceptors and one set of transfer parameters. The solid lines are given by the detailed theory of Eq. (9), where a distance dependent diffusion coefficient $D(R)$ has been included in the diffusional operator of Eq. (6). The electron transfer parameters are $J_0=60$ cm^{-1}, $\beta=1.15$ Å^{-1}, and $\Delta G=-0.5$ eV. Each curve has been convolved with a 50 ps Gaussian, a time scale similar to most time correlated single photon counting experiments. The radial distribution function used was calculated for a packing fraction of 50%, with molecules of 9.0 Å diam. The dashed lines are the best fits to these three curves obtained using the simple model [Eq. (7)], also convolved with a 50 ps Gaussian. The similarity of the two curves is actually quite good, and it is clear, at least for some values of the electron transfer parameters, that both the simple and detailed model can give nearly identical fits to experimental data. The crucial aspect, however, is the values for the parameters obtained by each model. The best fits of the simple model, as determined by least-squares analysis, were for parameters $J_0=52$ cm^{-1}, $\beta=2.1$ Å^{-1}, with a constant $\Delta G=-0.5$ eV. These values, while not unreasonable, are different than those used to gen-

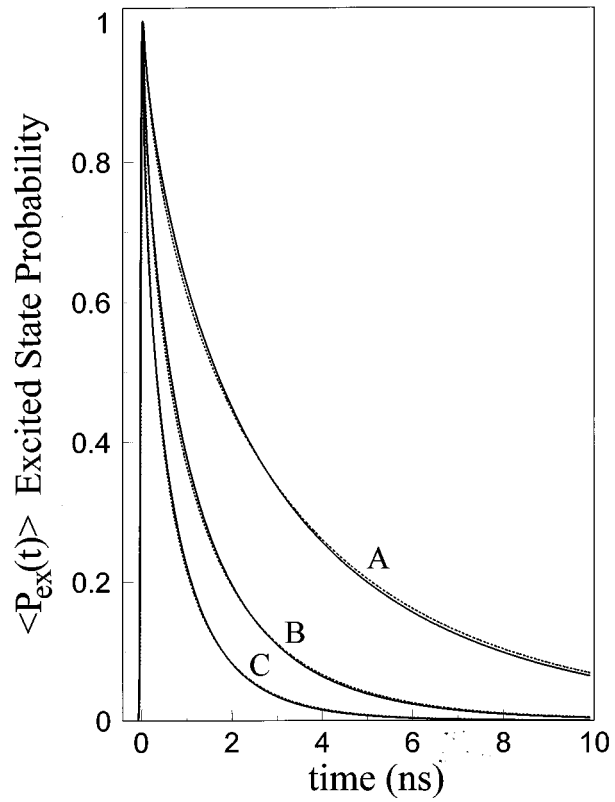

FIG. 4. Calculations of convolved $\langle P_{ex}(t)\rangle$ curves for three concentrations of electron acceptors. The solid lines are the detailed model including both $g(R)$ and $D(R)$, with $J_0=60$ cm^{-1}, $\beta=1.15$ Å^{-1}, $\Delta G=-0.5$ eV, for three acceptor concentrations. curve A is 0.1 M, curve B is 0.2 M, and C is 0.3 M. The dashed lines are the fits to these using the simple model with no solvent influences. All curves used $D=20.0$ Å^2/ns, and a donor–acceptor contact distance $R_m=9.0$ Å, with no fluorescence lifetime. For $g(R)$, the packing fraction was 0.5, and the particle diameter was 9.0 Å. The best fit parameters for the simple model were $J_0=52$ cm^{-1}, and $\beta=2.1$ Å^{-1}; ΔG was held constant. The instrument response for convolution was a 50 ps FWHM Gaussian. The solvent dielectric values are $\epsilon_{op}=2.0$, $\epsilon_s=5.0$.

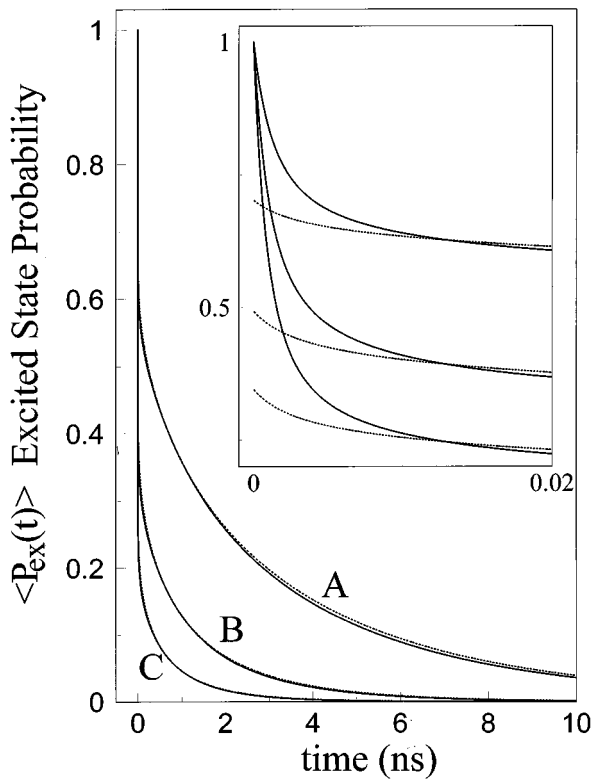

FIG. 5. Unconvolved excited state probability $\langle P_{ex}(t)\rangle$ for three concentrations, calculated with the detailed model, with attempted fits by the simple model. All parameters are the same as Fig. 4, except no convolution included.

erate the detailed model curves. This is particularly true of β. This ability of the simple model to reproduce convolved curves generated from the full detailed model was observed for several sets of transfer parameters. In every case, however, the parameters obtained by the simple model fits were significantly different than those used to generate the detailed model curves. Thus, while the simple model may be able to provide fits to some experimental systems, the values of the parameters obtained do not represent the physical reality of the molecular system. The values obtained for J_0 and β in this case are distorted by requiring them to additionally account for the solvent structure and hydrodynamic effect. For some sets of parameters, it was found that the continuum theory could not reproduce the detailed theory curves even with the 50 ps convolution.

In order to more rigorously test the models, comparisons were made between the simple and detailed models in the absence of a convolution with an instrument response. Using experimental methods such as fluorescence upconversion techniques[58] with roughly 100 fs time response, the influence of instrument response convolutions becomes less significant. In the limit of very short instrument response, the data must be fit by unconvolved $\langle P_{ex}(t)\rangle$ calculations. To compare the simple and detailed methods under these conditions, excited state curves were calculated using the full theory with a variety of physically reasonable transfer parameters. Fits to these detailed model curves were attempted using the simple model. In nearly every case, it was impossible to adequately reproduce the unconvolved $\langle P_{ex}(t)\rangle$ which included $g(R)$ and $D(R)$. The fast short-time behavior, coupled with the much slower long-time decay gives a functional shape which can not be produced when solvent structure and the hydrodynamic effect are not included. Figure 5 shows excited state curves for all the same conditions as Fig. 4, but without a convolution. The long time shape of the detailed model can be adequately reproduced, but the short time rapid decay cannot be simultaneously fit (shown in the inset). There are no values of the electron transfer parameters for which the simple model can match the detailed curves at all times. Thus, under certain conditions, the omission of $g(R)$ and $D(R)$ terms cannot only could lead to incorrect values of the transfer parameters, but can also prevent experimental data from being fit over the full range of times.

All of the detailed calculations were done using a solvent packing fraction of 0.5, with hard sphere repulsion. This is an approximate description of liquid structure. It is not, in general, possible to know the exact form of the solvent structure for a given system, and thus the form of $g(R)$ may have

significant error bars. The form of $g(R)$ will be affected by the choice of intermolecular potential. Whether the potential is assumed to be a step function (hard spheres), or some form of softer distance dependence (Lennard-Jones), $g(R)$ will have somewhat different magnitudes. Regardless of this uncertainty the inclusion of $g(R)$ is crucial. Even if values for the solvent structure are approximate, they will be closer to physically realistic conditions than if the solvent is considered to be uniform and unstructured. By making well educated approximations for the solvent density and molecular size, fairly accurate forms of the rdf can be generated.

IV. CONCLUDING REMARKS

The finite volume of solvent molecules plays a significant role in the rates and distributions of chemical reactions in solution. Among the most important effects are the solvent structure and the hydrodynamic effect. Previous theories modeling electron transfer have ignored these effects, assuming that the solvent is an isotropic, unstructured continuum. However, both $g(R)$ and $D(R)$ have been studied experimentally. The inclusion of $g(R)$ and $D(R)$ profoundly alter the time dependence of calculated charge transfer curves. The first of these effects, $g(R)$, gives rise to variations in local density at short distance. The most dramatic change is found at contact, where the local density can be several times greater than the average bulk density. Molecules separated by small distances are likely to react very swiftly, and calculations of the short time behavior of electron transfer systems will be markedly different than if the solvent is considered to be an unstructured continuum. In general, this change causes the rates of both forward and back electron transfer to be increased dramatically at short time. In addition, the hydrodynamic effect, $D(R)$, gives rise to a distance dependent diffusion term, which also changes the form of calculated electron transfer curves. The long time transfer rates, under conditions where diffusion is significant, are slowed considerably.

The simple model for electron transfer, based on an unstructured continuum solvent, gives a qualitatively correct description of through-solvent intermolecular photoinduced electron transfer. However, due to a lack of an accurate description of solvent structure and diffusion rates, the simple model improperly evaluates the physical parameters of the system. While it may be possible to fit experimental data using the continuum description of liquids, the values of the electron transfer parameters will be inaccurate.

The hard sphere model for $g(R)$ used in this paper is a reasonable description of liquid structure. A detailed analysis of its utility for understanding experimental results will be presented in a subsequent publication. For a small number of simple liquids, such as benzene, neutron scattering experiments have obtained direct measurements of the solvent rdf. Neutron scattering data show a softer repulsive potential than a hard sphere liquid, allowing a finite probability for two particles to approach closer than the sum of their van der Waals radii. Calculations of excited state probabilities were generated using both an experimental $g(R)$ and a properly parameterized PY hard sphere $g(R)$. The results of the calculations using the two forms of $g(R)$ were virtually identical, indicating the applicability of the hard sphere model to electron transfer dynamics in real liquids. These results and the analysis of experimental data using the methods presented here will be published soon.

The mathematical formalism required to include both the solvent structure and the hydrodynamic effect are relatively straightforward to implement. The changes to the simple, unstructured continuum theory can be accomplished using the methods given in this paper. In order to properly describe photoinduced electron transfer dynamics and to obtain physically reasonable transfer parameters, the effects of finite solvent volume must be included.

ACKNOWLEDGMENTS

This work was supported by the Department of Energy, Office of Basic Energy Sciences (Grant No. DE-FG03-84ER13251). The computers used in this work were provided by a grant from the National Science Foundation (Grant No. NSF-CHE-9408185).

[1] P. F. Barbara, G. C. Walker, and T. P. Smith, Science **256**, 975 (1992).
[2] T. Guarr and G. McLendon, Coordination Chem. Rev. **68**, 1 (1985).
[3] J. Cortes, H. Heitele, and J. Jortner, J. Phys. Chem. **98**, 2527 (1994).
[4] R. A. Marcus, Annu. Rev. Phys. Chem. **15**, 155 (1964).
[5] Y. Lin, R. C. Dorfman, and M. D. Fayer, J. Chem. Phys. **90**, 159 (1989).
[6] R. C. Dorfman, Y. Lin, and M. D. Fayer, J. Phys. Chem. **94**, 8007 (1990).
[7] R. C. Dorfman, thesis, Stanford University, 1992.
[8] A. I. Burshtein, Chem. Phys. Lett. **194**, 247 (1992).
[9] A. I. Burshtein, A. A. Zharikov, and N. V. Shokhirev, J. Chem. Phys. **96**, 1951 (1992).
[10] S. F. Swallen, K. Weidemaier, and M. D. Fayer, J. Phys. Chem. **99**, 1856 (1995).
[11] J. K. Percus and G. Y. Yevick, Phys. Rev. **120**, 1 (1958).
[12] E. Thiele, J. Chem. Phys. **39**, 474 (1963).
[13] M. S. Wertheim, Phys. Rev. Lett. **10**, 321 (1963).
[14] W. R. Smith and D. Henderson, Mol. Phys. **19**, 411 (1970).
[15] J. L. Lebowitz, Phys. Rev. **133A**, 895 (1964).
[16] L. Verlet and J. J. Weil, Phys. Rev. A **5**, 939 (1972).
[17] S. A. Rice, *Diffusion-Limited Reactions* (Elsevier, Amsterdam, 1985).
[18] R. Zwanzig, Adv. Chem. Phys. **15**, 325 (1969).
[19] J. M. Deutch and B. U. Felderhof, J. Chem. Phys. **59**, 1669 (1973).
[20] P. G. Wolynes and J. M. Deutch, J. Chem. Phys. **65**, 450 (1976).
[21] S. H. Northrup and J. T. Hynes, J. Chem. Phys. **71**, 871 (1979).
[22] M. V. Smoluchowski, Z. Phys. Chem. (Leipzig) **92**, 129 (1917).
[23] P. Debye, Trans. Electrochem. Soc. **82**, 265 (1942).
[24] M. D. Fayer, L. Song, S. F. Swallen, R. C. Dorfman, and K. Weidemaier, in *Ultrafast Dynamics of Chemical Systems*, edited by J. D. Simon (Kluwer Academic, Amsterdam, 1994).
[25] S. F. Swallen and M. D. Fayer, J. Phys. Chem. **103**, 8864 (1995).
[26] L. Song, S. F. Swallen, R. C. Dorfman, K. Weidemaier, and M. D. Fayer, J. Phys. Chem. **97**, 1374 (1993).
[27] F. C. Collins and G. E. Kimball, J. Colloid Sci. **4**, 425 (1949).
[28] S. Murata, M. Nishimura, S. Y. Matsuzaki, and M. Tachiya, Chem. Phys. Lett. **219**, 200 (1994).
[29] R. A. Marcus, J. Chem. Phys. **24**, 966 (1956).
[30] S. Murata, S. Y. Matsuzaki, and M. Tachiya, J. Phys. Chem. **99**, 5354 (1995).
[31] (a) M. Tachiya, Radiat. Phys. Chem. **21**, 167 (1993); (b) M. Inokuti and F. Hirayama, J. Chem. Phys. **43**, 1978 (1965).
[32] N. Agmon and J. J. Hopfield, J. Chem. Phys. **78**, 6947 (1983).
[33] W. H. Press, B. P. Flannery, S. A. Teukolsky, and W. T. Vetterling, *Numerical Recipes in C* (Cambridge University, Cambridge, 1988).
[34] E. Pines, D. Huppert, and N. Agmon, J. Chem. Phys. **88**, 5620 (1988).
[35] J. P. Hansen and I. R. McDonald, *Theory of Simple Liquids* (Academic, London, 1976).

[36] M. P. Allen and D. J. Tildesley, *Computer Simulation of Liquids* (Clarendon, Oxford, 1987).
[37] D. A. McQuarrie, *Statistical Mechanics* (Harper & Row, New York, 1976).
[38] C. J. Pings, in *Physics of Simple Liquids*, edited by J. S. Rowlinson and G. S. Rushbrooke (North-Holland, Amsterdam, 1968).
[39] J. E. Enderby, in *Physics of Simple Liquids*, edited by J. S. Rowlinson and G. S. Rushbrooke (North-Holland, Amsterdam, 1968).
[40] A. J. Greenfield, J. Wellendorf, and N. Wiser, Phys. Rev. A **4**, 1607 (1971).
[41] J. D. Weeks, D. Chandler, and H. C. Andersen, J. Chem. Phys. **54**, 5237 (1971).
[42] J. G. Kirkwood, J. Chem. Phys. **3**, 300 (1935).
[43] M. Born and M. S. Green, *A General Kinetic Theory of Liquids* (Cambridge University, Cambridge, 1949).
[44] J. M. J. van Leeuwen, J. Groeneveld, and J. de Boer, Physica **25**, 792 (1959).
[45] E. Meeron, J. Math. Phys. **1**, 192 (1960).
[46] L. Verlet, Nuovo Cimento **18**, 77 (1960).
[47] J. K. Percus, Phys. Rev. Lett. **8**, 462 (1962).
[48] G. J. Throop and R. J. Bearman, J. Chem. Phys. **42**, 2408 (1965).
[49] J. W. Perram, Mol. Phys. **30**, 1505 (1975).
[50] E. D. Glandt and D. A. Kofke, Mol. Phys. **64**, 125 (1988).
[51] G. J. Throop and R. J. Bearman, J. Chem. Phys. **44**, 1423 (1966).
[52] J. Talbot, A. Perera, and G. N. Patey, Mol. Phys. **70**, 285 (1990).
[53] F. Ghazi and M. Rigby, Mol. Phys. **62**, 1103 (1987).
[54] B. J. Alder, Phys. Rev. Lett. **12**, 367 (1964).
[55] P. Attard, J. Chem. Phys. **91**, 3083 (1989).
[56] P. Attard and G. Stell, Chem. Phys. Lett. **189**, 128 (1992).
[57] C. Miller, J. Phys. Chem. **95**, 877 (1991).
[58] D. D. Eads, B. G. Dismer, and G. R. Fleming, J. Chem. Phys. **93**, 1136 (1990).